Remote sensing detection of droughts in Amazonian forest canopies

Liana O. Anderson[1], Yadvinder Malhi[1], Luiz E. O. C. Aragão[2], Richard Ladle[3,4], Egidio Arai[5], Nicolas Barbier[6] and Oliver Phillips[7]

[1]Environmental Change Institute, School of Geography and Environment, Oxford University, Oxford OX1 3QY, UK; [2]School of Geography, University of Exeter, Devon EX4 4RJ, UK; [3]School of Geography and Environment, Oxford University, Oxford OX1 3QY, UK; [4]Department of Agricultural and Environmental Engineering, Federal University of Viçosa, Viçosa, Brazil; [5]Remote Sensing Division, National Institute for Space Research (INPE) Avenida dos Astronautas, 1758 Jardim da Granja, São José dos Campos, SP 12227-010, Brazil; [6]IRD-UMR Botanique et Bioinformatique de l'Architecture des Plantes (AMAP), Boulevard de la Lironde, TA A-51/PS2, F–34398 Montpellier Cedex 05, France; [7]Ecology and Global Change, School of Geography, University of Leeds, Leeds LS2 9JT, UK

Author for correspondence:
Liana O. Anderson
Tel: +44 1392 848556
Email: liana.anderson@ouce.ox.ac.uk

Received: *30 March 2010*
Accepted: *18 May 2010*

New Phytologist (2010) **187**: 733–750
doi: 10.1111/j.1469-8137.2010.03355.x

Key words: Amazon, climate change, drought, MODIS (moderate resolution imaging spectroradiometer), phenology, tree mortality, tropical forest, vegetation indices.

Summary

• Remote sensing data are a key tool to assess large forested areas, where limitations such as accessibility and lack of field measurements are prevalent. Here, we have analysed datasets from moderate resolution imaging spectroradiometer (MODIS) satellite measurements and field data to assess the impacts of the 2005 drought in Amazonia.

• We combined vegetation indices (VI) and climatological variables to evaluate the spatiotemporal patterns associated with the 2005 drought, and explore the relationships between remotely-sensed indices and forest inventory data on tree mortality.

• There were differences in results based on c4 and c5 MODIS products. C5 VI showed no spatial relationship with rainfall or aerosol optical depth; however, distinct regions responded significantly to the increased radiation in 2005. The increase in the Enhanced VI (EVI) during 2005 showed a significant positive relationship ($P < 0.07$) with the increase of tree mortality. By contrast, the normalized difference water index (NDWI) exhibited a significant negative relationship ($P < 0.09$) with tree mortality.

• Previous studies have suggested that the increase in EVI during the 2005 drought was associated with a positive response of forest photosynthesis to changes in the radiation income. We discuss the evidence that this increase could be related to structural changes in the canopy.

Introduction

Satellite-derived information is an attractive tool for vegetation monitoring at regional and global scales. It provides full coverage of large and remote areas on a regular basis over extended periods of time. Of the many remote sensing (RS) based techniques available for analysing vegetation dynamics, time-series analysis of vegetation indices (VIs) has become the most common approach for phenology and drought assessment.

The normalized difference vegetation index (NDVI) was originally generated based on the advanced very high resolution radiometer (AVHRR) images with a time-series of > 20 yr, being one of one of the most studied satellite-derived index (Tucker, 1979; Justice *et al.*, 1991, 2002). The NDVI is based on the differential reflection of vegetation in the red and near-infrared (NIR) spectra (green vegetation absorbs relatively more in the red and reflects considerably more in the NIR than in other spectral channels), and has been extensively used for ecosystem monitoring. However, a number of limitations have been identified in using the NDVI, including index saturation in closed canopies, and sensitivity to atmospheric aerosols and soil background (Di, 1991; Huete *et al.*, 1994; Wang *et al.*, 2003).

With the advances in technology, the acquisition of data across a larger number of channels and at higher spectral resolutions has become possible, leading to the development of new and improved indices (Liang, 2004). The enhanced vegetation index (EVI) was developed to minimize soil and atmospheric sensitivity observed in the NDVI by including the blue band for atmospheric correction (Huete *et al.*, 1994, 2002). For drought monitoring, the normalized difference water index (NDWI) has emerged as an index sensitive to changes in liquid water content in vegetation canopies (Gao, 1996). The NDWI uses NIR and short-wave infrared (SWIR) channels that are sensitive to changes in both canopy water content (which tends to absorb SWIR radiation) and spongy mesophyll in vegetation (details in Materials and Methods section).

In 2000, the moderate resolution imaging spectroradiometer (MODIS) onboard the Terra Earth Observation System satellite began acquiring images with improved radiometric, geometric rectification system and spatial resolution compared to the AVHRR (Justice *et al.*, 2002). The MODIS VI product (MOD13) encompasses two indices: the NDVI and the EVI (details in the Materials and Methods section). Available MODIS products undergo updates as the latest algorithms are applied to the instrument's data. A collection numbering scheme is used to differentiate among different reprocessing runs, where the highest number reflects the most recently improved or reliable version of the product. The latest collection, MOD13 c5, released in the beginning of 2007, incorporates improved input and data filtering, a modified compositing algorithm to select data acquired at the smaller view angles and a revised atmospheric correction.

In 2005 much of the Amazon region experienced a substantial drought (Aragão *et al.*, 2007; Marengo *et al.*, 2008). Some global climate model (GCM) studies suggest that global climate change could increase the frequency of drought in Amazonia, with effects on ecosystems and human populations (Cox *et al.*, 2008). Saleska *et al.* (2007) evaluated the anomalies in the EVI generated from the MODIS c4 collection during the driest quarter of 2005 (July–September) in relation to the long-term mean (2000–2006). Unexpectedly, they found a significant increase in the EVI during the peak of the climatological drought rather than the anticipated decline. This was interpreted as a possible increase in productivity during the drought period, and led to the tentative conclusions that the Amazon forest may be more resilient to droughts than previously thought. Samanta *et al.* (2010) have criticized this analysis and subsequent conclusion by evaluating the effects of the 2005 drought using the EVI c4 product (July 2000–September 2005) and the c5 product (July 2000–September 2008). The authors reported differences with respect to the area and intensity of the 2005 increase in the EVI between results obtained from the c4 and c5 product. Although they also observed an increase in the EVI c5 during the 2005 drought, the area was less extensive than in Saleska *et al.* (2007).

In contrast to RS data, field-based studies have generated contradictory results from the ones cited earlier. In an artificial drought experiment in a primary forest in east-central Amazonia, after only 2 yr of rainfall exclusion there was an observed decline in the surface and deep soil water content, affecting some species' photosynthetic capacity, thinning the canopy and decreasing stem radial growth of large trees (Nepstad *et al.*, 2002). An on-the-ground assessment of long-term forest plots following the 2005 Amazonian drought indicated that plots most affected by the rainfall suppression exhibited a decline in the rate of net aboveground biomass accumulation, and those losses were driven by occasionally large mortality increases and by widespread decline in growth (Phillips *et al.*, 2009). A detailed review on canopy responses to dry season and drought is presented by Asner & Alencar (2010).

The present study provides a new critical assessment of the effects of the 2005 drought on the Amazon closed canopies forests, using the MODIS VI c5 product. In addition to examining the EVI, we also investigate the NDVI and the water-sensitive index (NDWI) to explore the consistency among the three VIs. Furthermore, we compare results from the c5 product with those from the c4 product with two standardized datasets encompassing exactly the same time-series (2000–2006). Finally, we compare the remotely-sensed based analysis with field plot data on forest mortality responses to the 2005 drought. Specifically, we aim to address the following questions:

- Did canopy vegetation indices exhibit anomalous values during the 2005 Amazon drought?
- Are there substantial differences between the patterns observed in indices derived from the MODIS c4 and MODIS c5?
- Which climatological and atmospheric variables (rainfall, radiation and aerosol optical depth) show the strongest association with the patterns of change in the VIs?
- Is there any relationship between changes in remotely-sensed indices and changes in vegetation dynamics as recorded by long-term forest ecology plots?

Materials and Methods

Data preparation

Vegetation Indices (VIs) The VIs datasets are the MODIS VI c4 product (MOD13A2) and c5 product (MOD13A3). The standard MOD13A2 c4 and MOD13A3 c5 products include the spectral bands red (620–670 nm, band 1), NIR (841–876 nm, band 2), blue (459–479 nm, band 3) and SWIR (2105–2155 nm, band 7), and information about the pixel quality, sun zenith angle, view zenith angle and

relative azimuth angle. The NDVI and EVI are calculated from the individual bands as follows:

$$\mathrm{NDVI} = \frac{(\rho_{\mathrm{NIR}} - \rho_{\mathrm{Red}})}{(\rho_{\mathrm{NIR}} + \rho_{\mathrm{Red}})} \quad \text{Eqn 1}$$

$$\mathrm{EVI} = 2.5 \times \frac{\rho_{\mathrm{NIR}} - \rho_{\mathrm{Red}}}{\rho_{\mathrm{NIR}} + (6 \times \rho_{\mathrm{Red}} - 7.5 \times \rho_{\mathrm{Blue}}) + 1} \quad \text{Eqn 2}$$

(ρ_{NIR}, ρ_{Red} and ρ_{Blue} are the reflectance in the NIR, red and blue channels respectively; 2.5 is a gain factor, 6 and 7.5 are coefficients designed to correct for aerosol scattering and absorption and 1 is a canopy background adjustment) (Huete *et al.*, 1994, 1999).

Twelve tiles of MODIS images were acquired from March 2000 to December 2006. The MOD13A2 c4 is a 16-d composite product. Two images per month (16 d composite) is the standard format, except for October, which has only one image composite for the month. We acquired 144 images yr^{-1} with 1 km spatial resolution, or 984 images for the entire period for each band. Although in theory a maximum of 64 observations over a 16-d cycle can be achieved (multiple observations may exist for 1 d because of sensor orbit overlap), during the wet season in tropical regions the cloud-free count can be as low as zero. Therefore, we generated monthly images to increase the likelihood of cloud-free pixels, improve the quality of the data and to reduce the size of the dataset. Although we have not used the quality assurance (QA) data provided in the product for assisting the pixel selection, our methodology used the maximum NDVI technique, which is based on the selection of the highest NDVI pixel value of two 16-d images corresponding to each month for generating the monthly composited image. This approach ensures that cloudy and off-nadir pixels are less likely to be selected for the final monthly composite, and has been demonstrated to produce adequate results (Carreiras *et al.*, 2003).

The MOD13A3 c5 product is a monthly composite atmospherically corrected and nadir-adjusted dataset with 1 km spatial resolution. The MOD13A3 product is generated using the 1 km 16-d MODIS VI output. In addition to the quality control (QC) filter provided in the 16-d product, it uses a time-weighted average of the reflectance fields in the 16-d composited VI product that fall within a particular month and the ones that overlap in the beginning and end of each calendar month (Huete *et al.*, 1999). Therefore the monthly product has a higher quality standard than the 16-d product. We have not used the QA for selecting the monthly pixels used in each image, but anomalous negative values in the dataset located over forest areas were substituted by the average of a 3×3 pixels window.

The mosaics were generated using the MODIS reprojection tool software (MRT, 2008).

The NIR and SWIR monthly spectral bands for MOD13A2 c4 and MOD13A3 c5 products were then used to generate the NDWI for the entire time-series :

$$\mathrm{NDWI} = \frac{(\rho\mathrm{NIR} - \rho\mathrm{SWIR})}{(\rho\mathrm{NIR} + \rho\mathrm{SWIR})} \quad \text{Eqn 3}$$

(ρNIR and ρSWIR are the NIR and SWIR reflectance bands, respectively).

The NDWI, developed by Gao (1996), has the potential for canopy-level water content estimation (Zarco-Tejada & Ustin, 2001; Xiao *et al.*, 2002; Asner *et al.*, 2005). Compared with NDVI, SWIR-based indices are less sensitive to saturation (Roberts *et al.*, 1997), although they are also affected by leaf structure, leaf dry matter, canopy structure and leaf area index (LAI). The MODIS SWIR band has so far only been evaluated for vegetation water content for open canopy/cropland areas (Chen *et al.*, 2005; Cheng *et al.*, 2007) and for assessing canopy moisture content in selective logging (Koltunov *et al.*, 2009).

The Results and the Discussion sections of this study focus on the EVI and the NDWI because of the current scientific debate on the published analysis of the EVI and novelty of the application of NDWI. The NDVI results are presented in the main document, but figures are also available in the Supporting Information.

Rainfall data and solar radiation data To explore relationships between the VIs and drought, we used a monthly time-series (January 2000–December 2006) of the rainfall data derived from the tropical rainfall measuring mission (TRMM) (NASA, 2006), product 3B43 version 6, at 0.25° spatial resolution (details in the Supporting Information).

Monthly mean values of the total incoming radiation (January 2000–December 2006) were generated based on the 5-d, 0.4° gridded product from the GL/CPTEC model GL1.2. The solar radiation data ($\mathrm{W\ m}^{-2}$) are derived from visible band images from the satellite GOES-12, providing daily surface irradiation (Ceballos *et al.*, 2004).

Aerosol optical depth Aerosol optical depth (AOD) is a dimensionless measure of how many airborne particles (dust, cloud droplet, ice particles, biomass smoke, etc.) prevent the transmission of light. It varies from 0 to 1, where 0 corresponds to a completely transparent medium and 1 corresponds to high aerosol concentration. Data for AOD are available in the MODIS MOD08 level 3 c5 monthly product (Hubanks *et al.*, 2008). This is a $1 \times 1°$ gridded global dataset, computed from the complete set of daily files that span a particular month. We used the monthly mean and standard deviation from March 2000 to December 2006. Although not strictly a conventional climate variable, exploring AOD patterns enabled us to assess

whether there may be lingering atmospheric effects on VIs values.

Evergreen forest limits To avoid the false detections of anomalies owing to land-cover changes, we limited our analysis to areas which up to 2005 were known to be covered by forest. The 'evergreen' class of the TREES Vegetation Map (Eva *et al.*, 2004) was used as basis for the delimitation of the forested areas. The validation for this map by Eva *et al.* (2004) suggests the forest classes exhibited a good correlation with the reference data (r^2 = 0.97).

The TREES map was updated for deforested areas in the Brazilian Amazon by utilizing products from the program for the estimation of gross deforestation in the Brazilian Amazon (PRODES) (INPE, 2002) up to 2005. Although no validation estimate is presented in the methodological guidelines for the PRODES product (Câmara *et al.*, 2006), this dataset has been widely used by the scientific community. A 1-km buffer was generated around the deforestation polygons to minimize the effects of undetected deforested areas and to minimize spatial geo-correction problems between the two datasets.

The PRODES data were resampled to 1 km spatial resolution, to match the spatial resolution of the original TREES map (Fig. 1).

Tree mortality data The tree mortality data (number of individual trees that died) were derived from long-term forest inventory plots within the RAINFOR network (http://www.rainfor.org; Malhi *et al.*, 2002). The mortality rates were estimated based on the Sheil & May (1996) methodology and a census-interval correction was applied (Lewis *et al.*, 2004). For this study we looked at anomalies in tree mortality, which were calculated as the difference in rate of mortality between the drought and pre-drought period.

Nineteen sites located on the Amazon primary forest were used in this analysis (Fig. 1) (see Phillips *et al.*, 2009, 2010). Field plots located on the same site and measured with the same census interval dates were aggregated to decrease possible effects of spatial autocorrelation (Table 1).

Data analyses

Temporal patterns To understand the temporal trends for the region, we generated a time-series based on data averaged over all the Amazon forest pixels. Two analyses were carried out. First, monthly anomalies (z-score, Eqn 4) for the entire dataset (VIs, rainfall, radiation, AOD) were used to evaluate changes in the pattern during 2005. The z-score for a variable is calculated as follows:

$$z_m = \frac{(\overline{X}_m - \overline{\langle X_m \rangle})}{\sigma(\overline{X}_m)} \qquad \text{Eqn 4}$$

(X is the analyzed variable; $\overline{X}_m$ is the spatial average value for each month m; $\overline{\langle X_m \rangle}$ is the mean of $\overline{X}_m$over that same month of the year over the multi-year dataset; and $\sigma(\overline{X}_m)$is the standard deviation of $\overline{X}_m$for the total time series over that same month of the year).

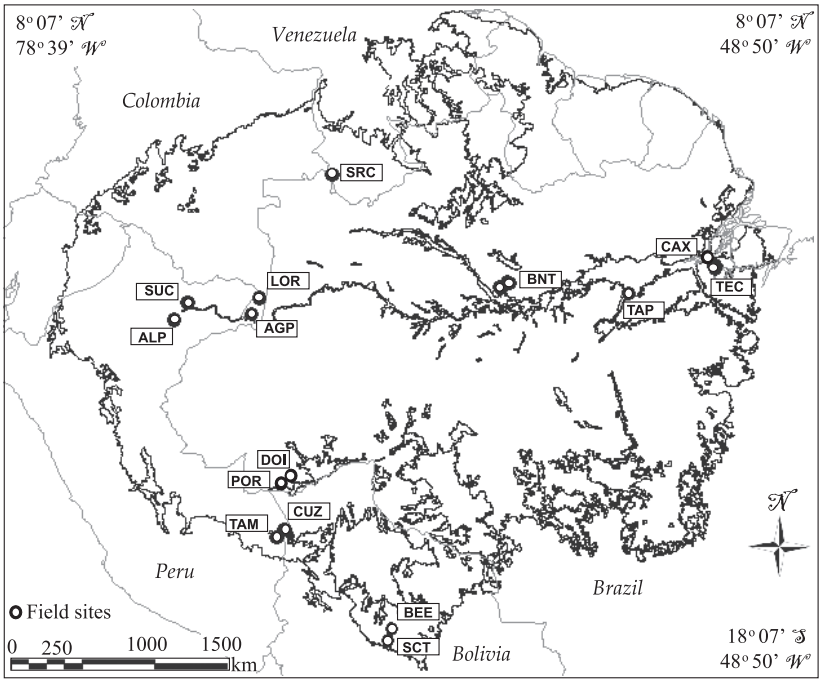

Fig. 1 Location of the relevant RAINFOR field sites. See Table 1 for details.

Table 1 Plot attributes and field data

Country	Plot code	Latitude	Longitude	Tree mortality anomaly in 2005
Colombia	AGP-01, AGP-02	−3.72	−70.31	0.64
Peru	ALP-11, ALP-12, ALP-21, ALP-22	−3.95	−73.44	−1.30
Bolivia	BEE-01, BEE-05	−16.53	−64.58	−0.83
Brazil	BNT-01, BNT-02, BNT-03	−2.63	−60.17	0.24
Brazil	CAX-08	−1.86	−51.44	0.23
Peru	CUZ-01, CUZ-02, CUZ-03, CUZ-04	−12.5	−68.97	1.61
Brazil	DOI-01, DOI-02	−10.33	−68.18	2.323
Colombia	LOR-01, LOR-02	−3.06	−69.99	−0.06
Brazil	POR-01, POR-02	−10.49	−68.46	0.621
Venezuela	SCR-04D, SCR-05D	1.93	−67.04	−0.31
Bolivia	SCT-01, SCT-06	−17	−64.77	1.07
Peru	SUC-01, SUC-02	−3.25	−72.91	−0.96
Peru	SUC-03, SUC-04	−3.26	−72.9	−0.23
Peru	TAM-01, TAM-02, TAM-05, TAM-06, TAM-07	−12.84	−69.28	0.04
Peru	TAM-08	−12.83	−69.27	0.51
Brazil	TAP-80	−2.9	−54.95	0.82
Brazil	TEC-01	−1.71	−51.46	−1.07
Brazil	TEC-02, TEC-03, TEC-04, TEC-06	−1.73	−51.5	0.22
Brazil	TEM-03, TEM-04, TEM-05, TEM-06	−2.44	−59.78	0.83

The z-score indicates how far and in what direction that item deviates from its mean, expressed in units of its distribution standard deviation. Therefore, the z-score values were used to specify the relative statistical location of each monthly value within the population distribution of 6 yr. Any z-values between 1 and −1 (i.e. within 1 standard deviation of the mean) are considered to represent normal variation in the data. Confidence intervals were established as follows: $P = 0.1$ $-1.65 \leq z\text{-score} \geq 1.65$; $P = 0.05$ $-1.96 \leq z\text{-score} \geq 1.96$; and $P = 0.01$ $-2.57 \leq z\text{-score} \geq 2.57$ (Lee & Wong, 2001).

Second, linear regression analyses were carried out to test how monthly mean values of all pixels that fall within the forest limits of the dependent variables, the MOD13A3 c5 VIs, temporally relate to rainfall, radiation and AOD. Pearson's correlation indices of the monthly data and lagged response of the VIs (the VIs is always lagging the climate signal) were tested and the coefficient of determination (r^2), correlation coefficient (r) and standard error determined.

Spatial patterns Monthly anomalies (Eqn 4) for VIs and climatological variables were calculated on a pixel-by-pixel basis. Two analyses were then carried out. First, we explored the spatial pattern of the anomalous regions for all the variables. Months that presented stronger anomalies during 2005 in the temporal basin-wide analysis (see the preceding section, 'Temporal patterns') were selected for explicit mapping. To reduce the noise in the data, the 1 km VIs anomalies were resampled to 0.25° using an aggregated resampling algorithm that averages the values of all pixels included in the 0.25° output pixel size.

Second, a Pearson correlation analysis was performed between the anomalies of the three VIs and the anomalies of the climatic variables. For each pixel, the maximum positive or negative value of the correlation coefficient (r) within a lag window of 6 months (VIs always lagging climate signal) was plotted. Complementary maps of the time lag were also plotted showing for each pixel the month that corresponds with maximum correlation. Lag time maps were not generated for the AOD, as we investigated only the direct effects of this variable on the VIs anomalies. To perform this analysis we used the same resampling algorithm as described earlier, resampling the 1 km VIs to match the same spatial resolution of the climatological variables.

Tree mortality data and vegetation indices The re-census of most of the plots occurred in 2006 (some plots were remeasured in 2005), after the drought had ended and at a similar time of year to previous censuses to minimize possible hydrostatic effects of wood shrink–swell. Hence the enhanced tree mortality observed in 2006 (i.e. anomalies in mortality) is likely to have occurred during or within a few months of the drought (Phillips *et al.*, 2009). In this study we suggest that trees that died from the 2005 drought first suffered from hydric stress and increased leaf shedding because of the anomalous dry period. As many of the trees died standing, the increased number of dead trees dying in the 2005 period may also be an indicator, in relative terms, of an increased number of trees that responded to the event by dropping their leaves.

We collected VIs anomalies data for 1 km pixels corresponding to the field plot location on the 1 km VIs anomalies (c5) for the 2005 driest period (June–September). The sites from which most of the field data are derived represents large areas of homogeneous forest (Anderson *et al.*, 2009), giving confidence in the VIs anomalies data

acquired. For sites that include more than one field plot (Table 1), the average value of the VIs anomalies was used.

Pearson correlation analyses were carried out between the anomaly in tree mortality data and vegetation indices anomalies. Significant correlations at 90% confidence were plotted and the coefficient of determination (r^2) and correlation coefficients (r) were determined.

Results

Temporal patterns

The anomalies (averaged over the whole region) for rainfall, solar radiation, AOD and the three VIs are presented in Fig. 2. Although the averaging over the region may hide strong subregional anomalies (e.g. some areas of Amazonia

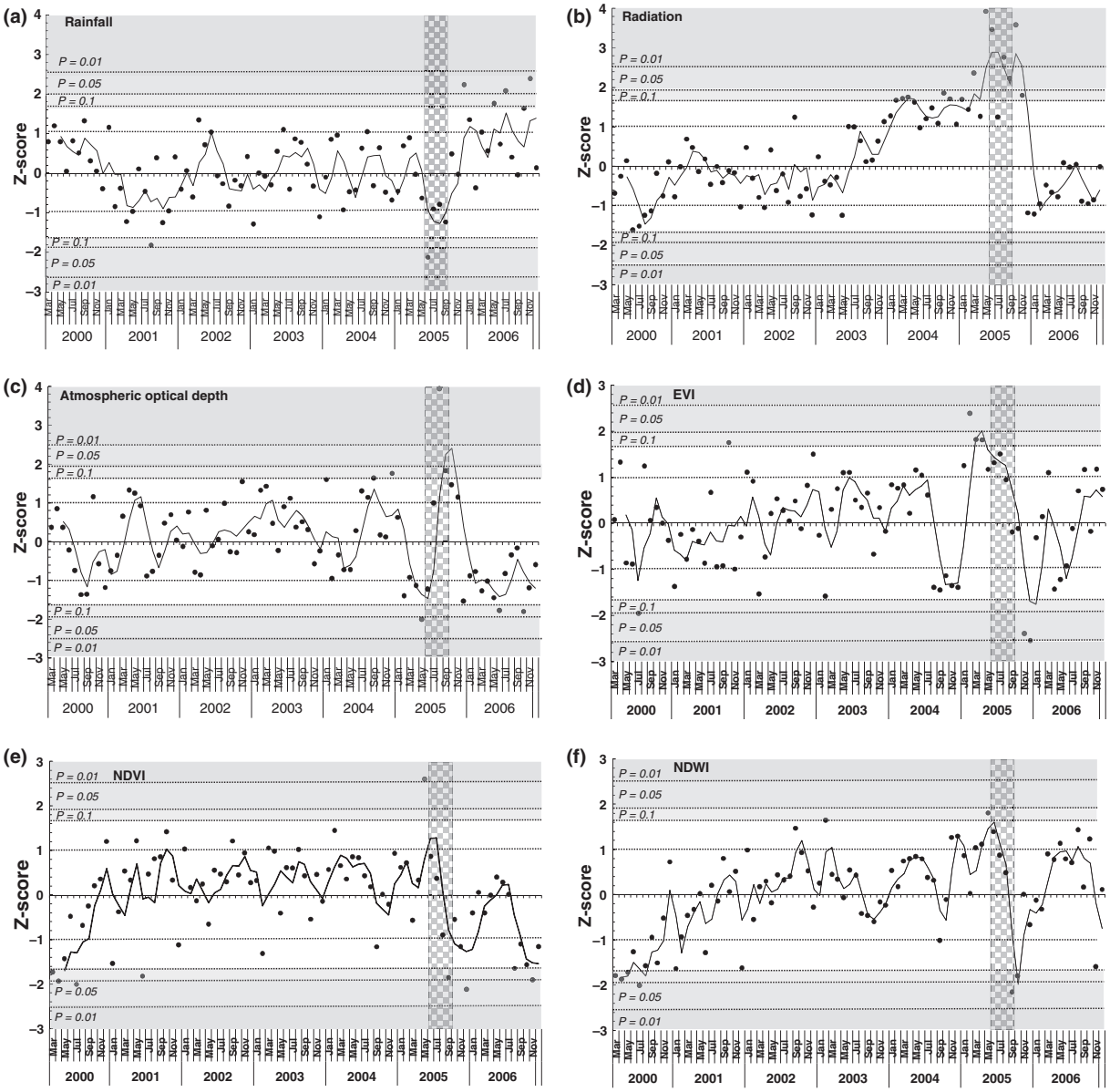

Fig. 2 Monthly time-series based on data averaged over all Amazon evergreen forest pixels, as identified in the limit generated in this study. The start of the data record is January 2000 for rainfall and radiation and March 2000 for the Terra MODIS (moderate resolution imaging spectroradiometer) products. (a) Rainfall from the tropical rainfall measuring mission (TRMM). (b) Radiation from the GL1.2/CPTEC model. (c) Aerosol optical depth (AOD) from MODIS MOD-08 level 3 collection 5 product. Vegetation indices from MOD13A3 collection 5 product (d) enhanced vegetation index (EVI), (e) normalized difference vegetation index (NDVI) and (f) normalized difference water index (NDWI). The shaded vertical bar denotes the 2005 drought period. Horizontal dashed lines represent significance level as shown.

being wetter when others undergo drought), this general evaluation is useful to highlight general relationships among the datasets.

Over the period 2001–2003 most of the anomalies were not significant at 90% confidence. By contrast, 2004–2006 exhibited higher amplitude anomalies, particularly the period 2004–2005. Specifically, we observed a persistence of negative anomalies in the rainfall from June to October 2005 and significant positive rainfall anomalies in much of May to July 2006 ($P = 0.1$) (Fig. 2a). Very strong increasingly significant positive anomalies in solar radiation were detected from May to November 2005 ($P = 0.01$), with a strong decrease from December 2005 onward (Fig. 2b). The AOD data exhibited two positive peaks (July–September in both 2004 and 2005) and negative peaks in March–June 2005 ($P = 0.05$) and 2006 ($P = 0.1$) (Fig. 2c).

The three VIs from the two collections showed anomalies outside the one z-score range in the time-series (Fig. 2d–f). Overall there was surprisingly little relation at this scale between the c4 and c5 products (see the Supporting Information, Fig. S1). Higher intermonthly variation was observed in the c4 than in c5, possibly because of the more simplistic rationale adopted (the maximum NDVI approach) for generating the monthly composites (see the Discussion section). However, it is likely that the biggest contribution to the differences between the two datasets is the refinements in the c5 algorithms (Didan & Huete, 2006). We can therefore corroborate the conclusion from Samanta *et al.* (2010), that results derived from c4 products should be treated with caution, which has implications with respect to the interpretation of previously published results (Myneni *et al.*, 2007; Saleska *et al.*, 2007). Henceforth, we focus our analysis on the c5 collection, which we interpreted as the more robust dataset.

The three VIs presented an increase in the positive anomalies in the months preceding or at the beginning of the 2005 drought, corresponding to the period when the strongest positive anomalies in VIs were observed in the temporal series.

A summary of the regression analysis of the basin-wide averaged VIs c5 with the climatological variables is presented in Table 2. Both NDVI and NDWI showed a significant relationship with rainfall for the same month, and with the most significant relationship at zero time lag. Interestingly, EVI showed the opposite pattern: no relationship with rainfall for the same month, and stronger correlations with 1 month and 2 months lag. All three VIs were negatively correlated with rainfall ($P < 0.001$). Positive correlations between the VIs and radiation were observed, but only EVI gave stronger lagged correlation with this variable. Finally, only EVI ($P < 0.001$) and NDVI ($P < 0.01$) were significantly correlated with AOD.

The results of the temporal patterns can be summarized as a detection of a drought event, during which radiation peaked. Differences emerged from VI product c4 and c5. We interpreted c5 as more robust product and therefore any analyses based on previous products should be treated with caution.

Table 2 Coefficient of determination (r^2) of the Pearson correlation among moderate resolution imaging spectroradiometer (MODIS) vegetation indices, solar radiation and rainfall

	Same month	1 month lag	2 months lag
Rainfall			
EVI	–	0.28**	0.62**
NDVI	0.55**	0.31**	–
NDWI	0.24**	0.16**	–
Radiation			
EVI	0.29**	0.62**	0.57**
NDVI	0.29**	–	–
NDWI	0.1*	–	–
			–
AOD			
EVI	0.36**	0.57**	0.36**
NDVI	0.1*	–	–
NDWI	–	–	–

AOD, aerosol optical depth; EVI, enhanced vegetation index; NDVI, normalized difference vegetation index; NDWI, normalized difference water index.
*, $P < 0.01$; **, $P < 0.001$. The equations are provided in Supporting Information Table S1.

Climatological variables anomalies Rainfall anomaly maps were produced for the period that exhibited marked anomalies (May–September 2005) (Fig. 3). May to September was dominated by negative anomalies, and the largest region affected by the decrease of the rainfall was observed in July. The Western Amazon region consistently presented negative anomalies in 2005, although eastern regions were also affected.

Radiation anomalies exhibited mainly positive values for all months (Fig. 4), peaking in May, June and September.

Aerosol optical depth anomaly maps were produced for the month that presented larger areas of significant anomalies (July–September) (Fig. S2). A markedly large and significant positive anomaly was observed in August in the central Amazon, coinciding with the course of the main rivers (Amazon and Negro rivers) possibly owing to seasonally exposed mud-banks. Negative homogeneous regions were observed in September, covering southern Amazonia.

In summary, there were positive and negative rainfall anomalies in 2005 varying in space and time; radiation peaked in the dry season and AOD positive anomalies coincided with the course of the main rivers.

Vegetation indices anomalies Significant positive and negative anomalies in the three VIs were observed only for 2005. The spatial results for the EVI c4 observed in this study (Fig. S3) is similar to that reported by Saleska *et al.* (2007), with most of the positive anomalies detected in August.

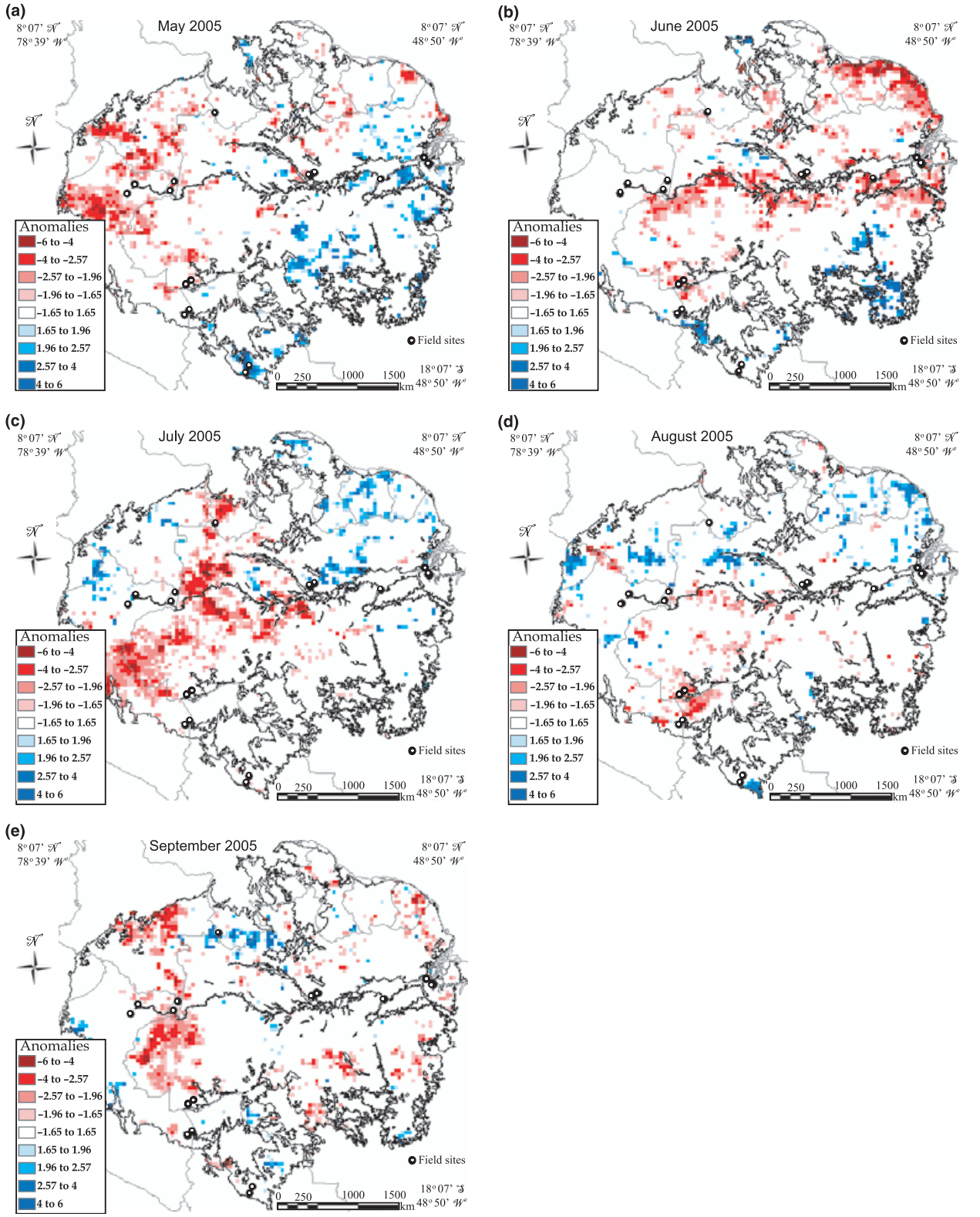

Fig. 3 Rainfall monthly anomalies in 2005. (a) May, (b) June, (c) July, (d) August and (e) September. The anomalies intervals are divided as follows: $P \leq 0.01$ *z*-score = ± 2.57, $P \leq 0.05$ *z*-score = ± 1.96, $P \leq 0.1$ *z*-score = ± 1.65.

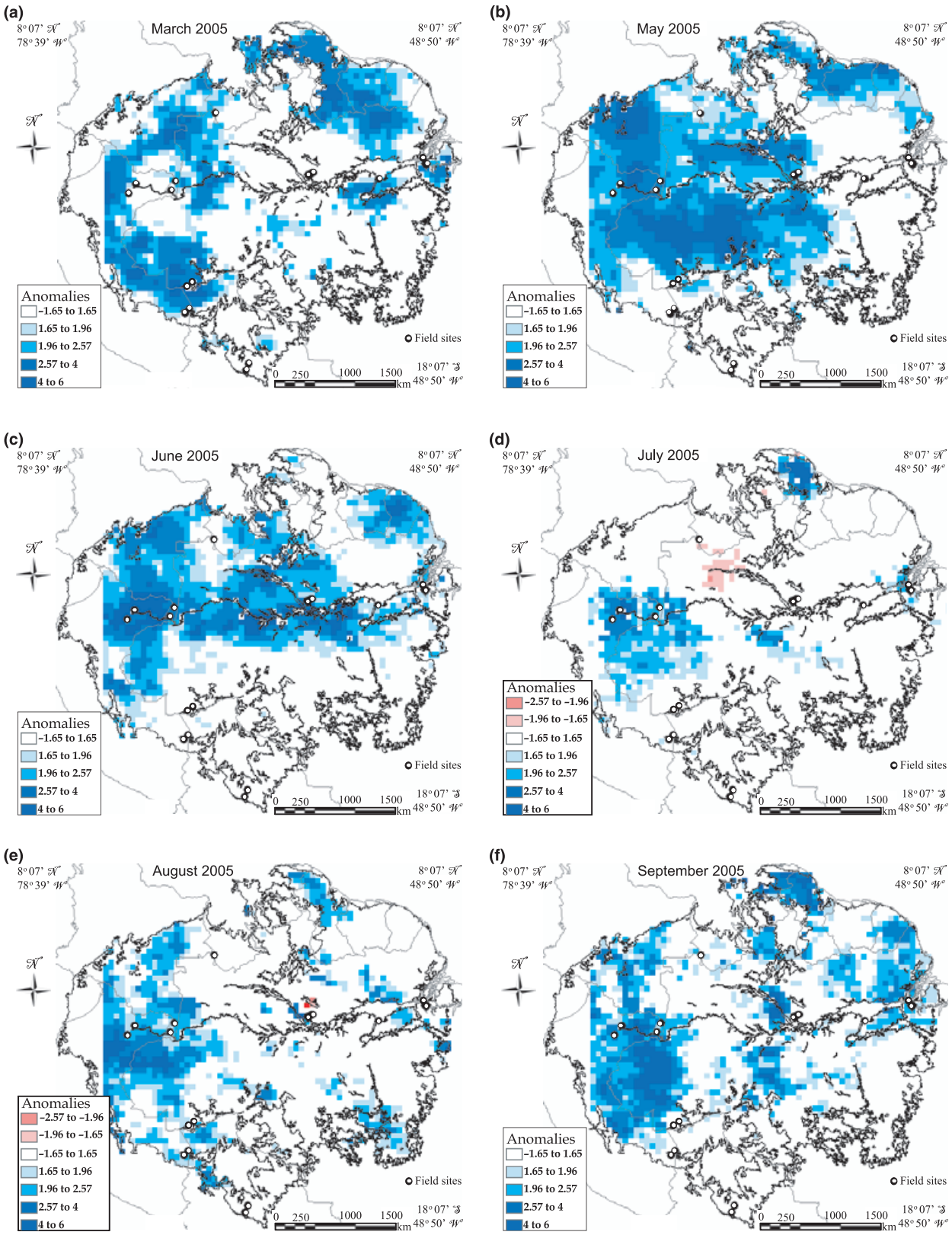

Fig. 4 Radiation monthly anomalies in 2005. (a) March, (b) May, (c) June, (d) July, (e) August and (f) September. The anomalies intervals are divided as follows: $P \leq 0.01$ z-score = ± 2.57, $P \leq 0.05$ z-score = ± 1.96, $P \leq 0.1$ z-score = ± 1.65.

The EVI c5 showed positive anomalous patterns from April to July 2005 (Fig. 5). Central and western regions of the forest presented a homogeneous pattern of positive anomalies. Negative anomalies dominated the EVI c5 for November and December 2005.

The NDVI c5 anomalies showed, in general, a predominance of negative anomalies during September, November and December 2005 (Fig. S4). A significant negative anomalous pattern was observed in the south-west region in September 2005. In November 2005, the NDVI c5 did not present any large region of anomalies (Fig. S4b). Interestingly, December 2005 presented large and homogeneous areas of negative anomalies in different regions (Fig. S4c).

As NDWI is related to moisture in the canopy, negative anomalies, indicating 'water stress', could be expected for 2005. However, the NDWI c5 gave predominately positive anomalies (Fig. 6). Interestingly, there was a marked pattern of positive anomalies in June in central and western Amazonia. Although at first this result suggests that NDWI did not capture the water stress, it is also possible that the water-stressed leaves were dropped and therefore NDWI was detecting the water content in the lower canopy. Despite the observed differences, in the anomalous trend between c5 NDWI and NDVI, both indices exhibited similar spatial pattern and negative anomalies in September 2005 (Figs 4d, S4a).

In summary, EVI and NDWI anomalous spatial patterns exhibit small areas of significant positive anomalies in the predrought period, and, like NDVI, they presented small areas with significant negative anomalies after September 2005.

Correlation between climatological and vegetation indices anomalies The maximum Pearson correlation between EVI and NDWI and the rainfall and radiation is presented in Fig. 7. The maximum Pearson correlation between the VIs anomalies and the AOD anomalies, the relationships between NDVI and the rainfall and radiation and the time lag complementary maps for the three VIs are presented in Figs S5–S7).

A longitudinal transect south of the Amazon river emerged as a region with significant negative correlation ($r = -0.4$ to -0.2) between the rainfall and EVI anomalies (i.e. unusually low rainfall = unusually high EVI) (Fig. 7a). In addition, from the Guyana shield to central Amazonia to Venezuela and Colombia, positive anomalies were predominant ($r = 0.1$–0.4) (i.e. unusually low rainfall = unusually low EVI) (Fig. 7a). Despite these spatial patterns between anomalies in the EVI and rainfall, the time lag map (Fig. S7a) showed no consistent homogeneous region, suggesting that the highlighted regions with similar correlations did not respond similarly to the same event. Conversely, the time lag map for anomalies in the EVI and radiation showed homogeneous and consistent large areas responding similarly (Fig. 7b). The AOD relationships showed no strong spatial pattern, and therefore it is likely that anomalies in the aerosols were not associated with anomalies detected in the EVI, indicating that c5 removes atmospheric effects of the temporal dataset (Fig. S5a).

Negative relationships between NDVI c5 and rainfall anomalies in the north-western Brazilian Amazon region ($r = -0.6$ up to -0.1) showed the highest correlation at 1–3 months lag and this pattern was similar in the central-eastern region, whereas the negative correlations in this area were associated with 1-month lag time (Fig. S6). Areas with positive relationships were very scattered in magnitude of lag time (Fig. S7c). Overall, anomalies in NDVI appeared to be more consistent with anomalies in the rainfall than EVI anomalies, although this was observed only for the negative correlations. There was no strong spatial pattern in the AOD relationship with the NDVI (Fig. S5b).

Regions affected by the 2005 drought were dominated by negative relationships between the NDWI and rainfall, similar to the other two VIs (Figs 7c, S7e). Both NDWI and radiation showed large homogeneous regions with positive correlations and smaller regions with negative relationships (Figs 7d, S7F). The AOD maximum correlation map showed a higher correlation coefficient than the other two VIs, but pixels with high correlation were very scattered.

The relationships of the VIs c5 and rainfall were positive and negative varying in space and time, and covering small areas, while radiation anomalies relationships covered continuous areas and were persistent in time.

Tree mortality data and the vegetation indices Weak but significant correlation between tree mortality anomalies and the anomalies in EVI and NDWI for June, July and August 2005 ($P < 0.1$) were observed (Fig. 8).

The June and July EVI anomaly exhibited positive correlation and the August NDWI anomaly exhibited a negative correlation with tree mortality anomaly. The greatest anomalies in tree mortality rates were found at sites in southern and western Amazonia (e.g. CUZ, DOI, LOR, POR, SCT and TAM-08). Positive anomalies in EVI and negative anomalies in NDWI were observed in those sites with higher tree mortality. The trend shows higher EVI and lower NDWI anomalies in sites with increased tree mortality.

Discussion

Temporal patterns

Climate Several interesting patterns in the climatological data and in the VIs emerged despite the potentially obscuring effects of basin-wide pixel-averaging. For example, the averaging analysis was able to capture the decline in rainfall after May 2005 ($P = 0.05$). It is interesting that although

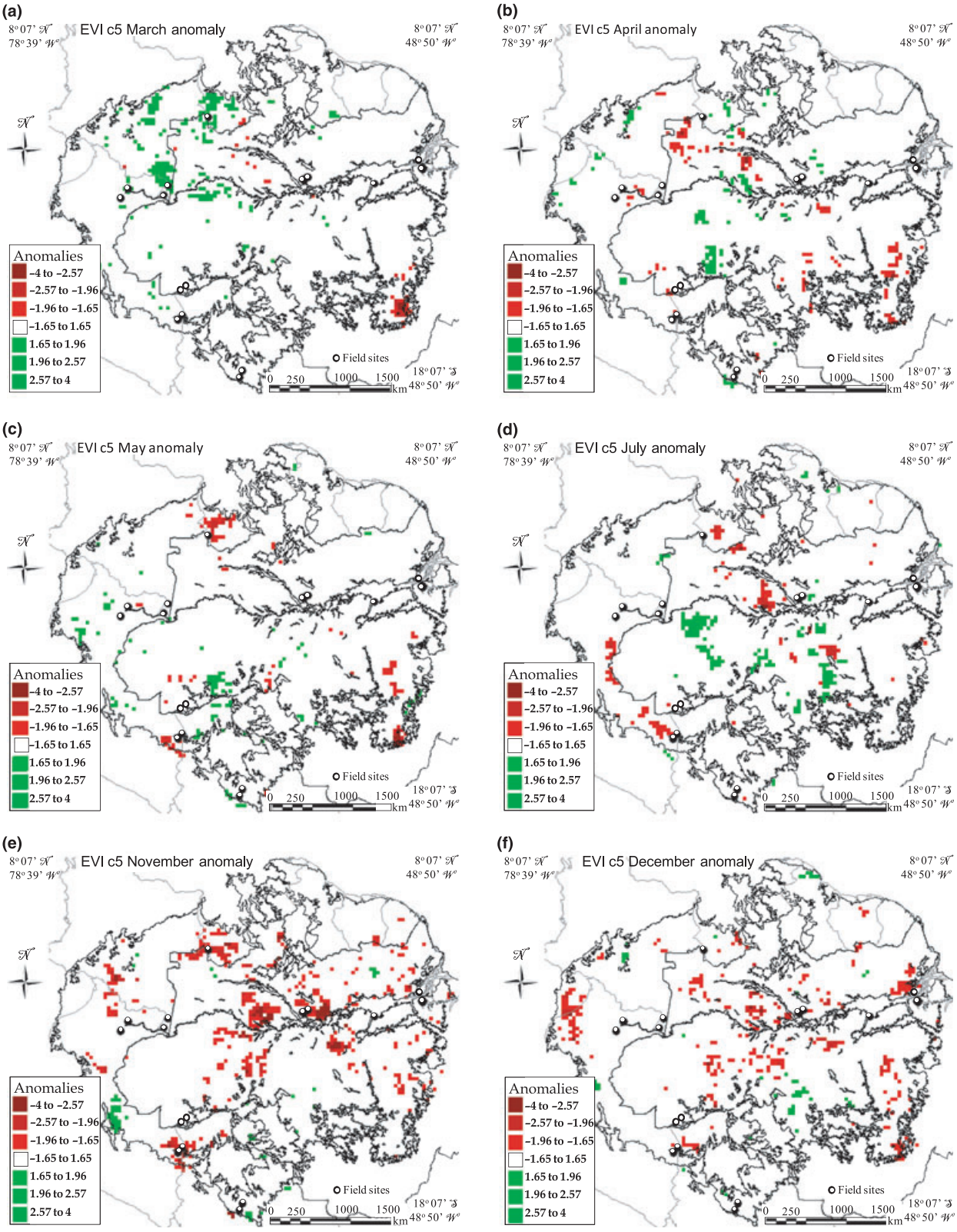

Fig. 5 Enhanced vegetation indices (EVIs) c5 monthly anomalies in 2005. (a) March, (b) April, (c) May, (d) July, (e) November and (f) December. The anomalies intervals are divided as follows: $P \leq 0.01$ *z*-score = ± 2.57, $P \leq 0.05$ *z*-score = ± 1.96, $P \leq 0.1$ *z*-score = ± 1.65.

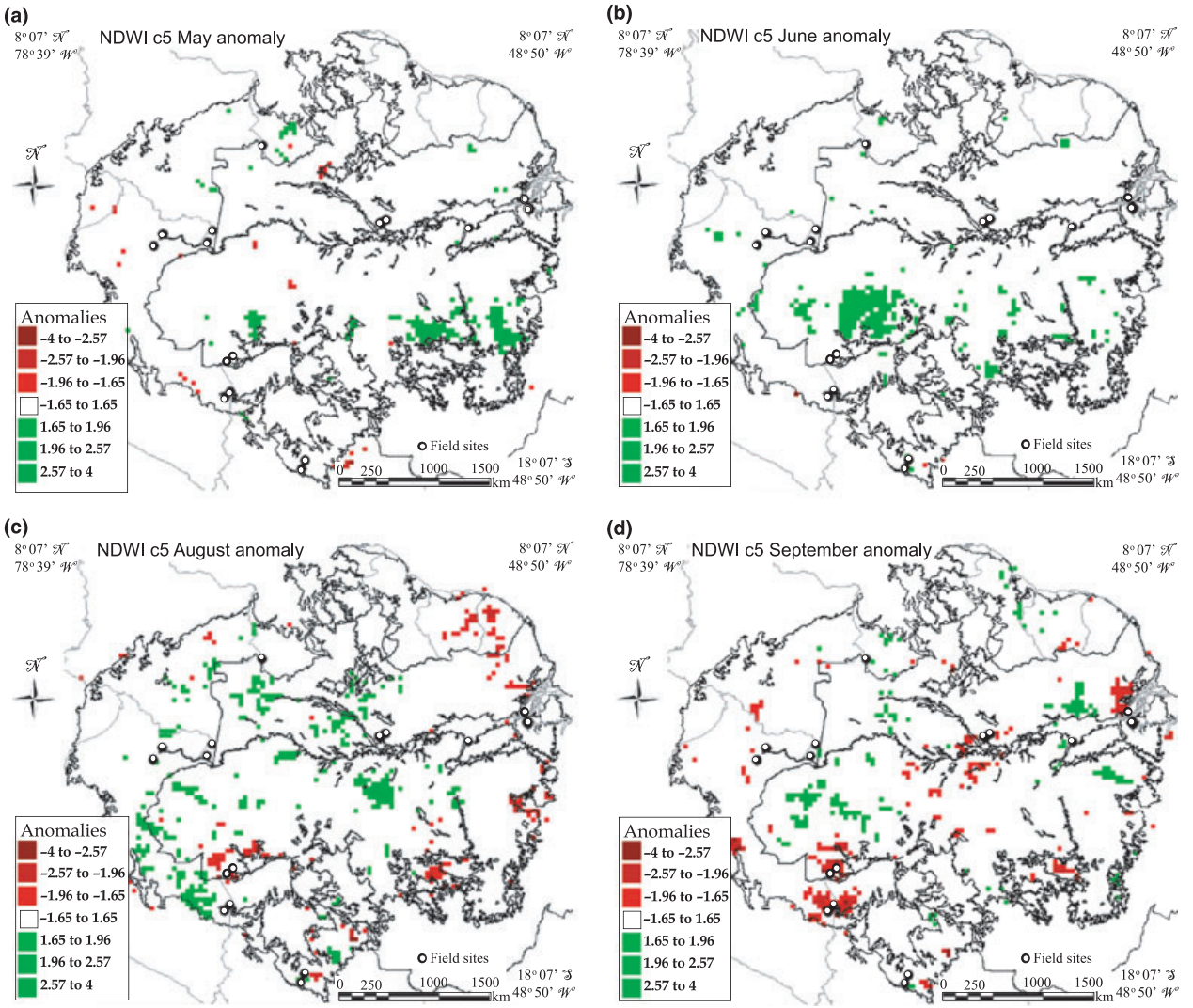

Fig. 6 Normalized difference water index (NDWI) c5 monthly anomalous in 2005. (a) May, (b) June, (c) August and (d) September. The anomalies intervals are divided as follows: $P \leq 0.01$ *z*-score = ± 2.57, $P \leq 0.05$ *z*-score = ± 1.96, $P \leq 0.1$ *z*-score = ± 1.65.

only May exhibited significant negative anomaly at monthly resolution, the reported duration of the drought was longer (Aragão *et al.*, 2007; Marengo *et al.*, 2008) and, in this basin-wide analysis, was apparent as the persistence of negative anomalies through much of 2005.

The persistence of positive anomalies in the total incoming radiation from the beginning of 2004 until November 2005 (Fig. 2b) could indicate a prolonged period of increased insolation. However, Samanta *et al.* (2010) reported a decrease in the 2005 short-wave and diffuse photosynthetically active radiation (PAR) in relation to the 2000–2004 period. Such dissimilarity could be related to the differences in the time-series used in this study and in Samanta *et al.* (2010), and the fact that the GL1.2 model does not consider aerosols (Ceballos *et al.*, 2004).

Although radiation and aerosols generally show opposite trends (Schafer *et al.*, 2002; Koren *et al.*, 2004), an increasing trend in the annual aerosol optical depth over the Amazon has been reported, owing to the increase in fires in this region (Koren *et al.*, 2007). This was also detected in this study as the positive anomalies signal in AOD during 2001 and 2003–2005 (Fig. 2c).

Perhaps the most interesting pattern to emerge during the 2005 drought period was that radiation peaks as rainfall and AOD show their lowest values, the latter with a slight lag. The increase in radiation is related to a decrease in cloud cover (Li *et al.*, 2006) while the increase in AOD appears to be synchronized with the anomalous peak in fires over primary forest during the same period (Aragão *et al.*, 2007). By contrast, rainfall exhibits persistency of significant positive anomalies during 2006 with an immediate decrease in radiation and AOD. The decrease of AOD might be explained by aerosol washout by precipitation (Andreae *et al.*, 2004).

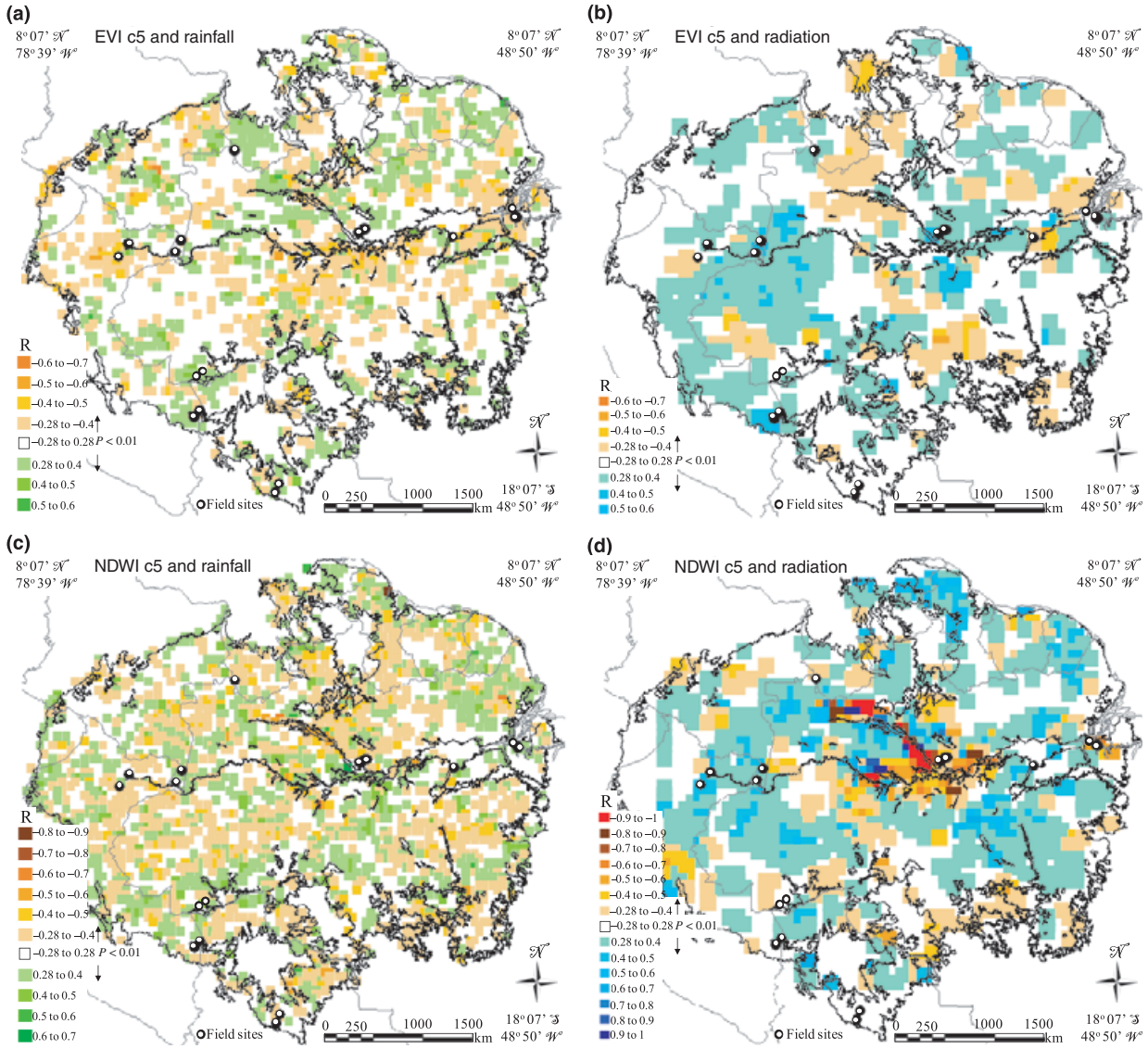

Fig. 7 Maps of maximum Pearson correlation (within 6 months time lag) between the vegetation indices anomalies (enhanced vegetation index (EVI) and normalized difference water index (NDWI) c5) and the rainfall and radiation anomalies. (a) EVI and rainfall anomalies, (b) EVI and radiation anomalies, (c) NDWI and rainfall anomalies and (d) NDWI and radiation anomalies. Critical value of the Pearson product-moment correlation coefficient is 0.284 (P = 0.01). (see the Supporting Information, Fig. S6 for NDVI results). The maximum correlation map between the VIs anomalies and aerosol optical depth (AOD) anomalies is presented in Fig. S5. The time lag complimentary maps for the maximum correlation are presented in Fig. S7.

Vegetation indices Although in principle the preprocessing of both c4 and c5 VIs products should produce a cloud-free image, different approaches for generating monthly composites affect the final image (Carreiras *et al.*, 2003; Vancutsem & Defourny, 2009). For example, Poulter & Cramer (2009) found that the MODIS LAI 8-d c5 is particularly sensitive to the methods used for generating monthly images. Conversely, they showed that the 16-d VI product c5 was less sensitive to additional filters as the product itself already filters for moderate-to-high aerosol concentrations, clouds and shadows. Therefore, by using the monthly VI c5 product in our analysis, few effects of clouds and aerosols were expected.

Myneni *et al.* (2007) evaluated a time-series of monthly LAI c4 averaged over all Amazon rainforest pixels and found that the phenological cycle peaks before solar radiation peaks in a timed seasonality. Huete *et al.* (2006), assessing the EVI c4, also found that sunlight may exert more influence than rainfall on rainforest phenology and productivity. Asner & Alencar (2010), analyzing > 300

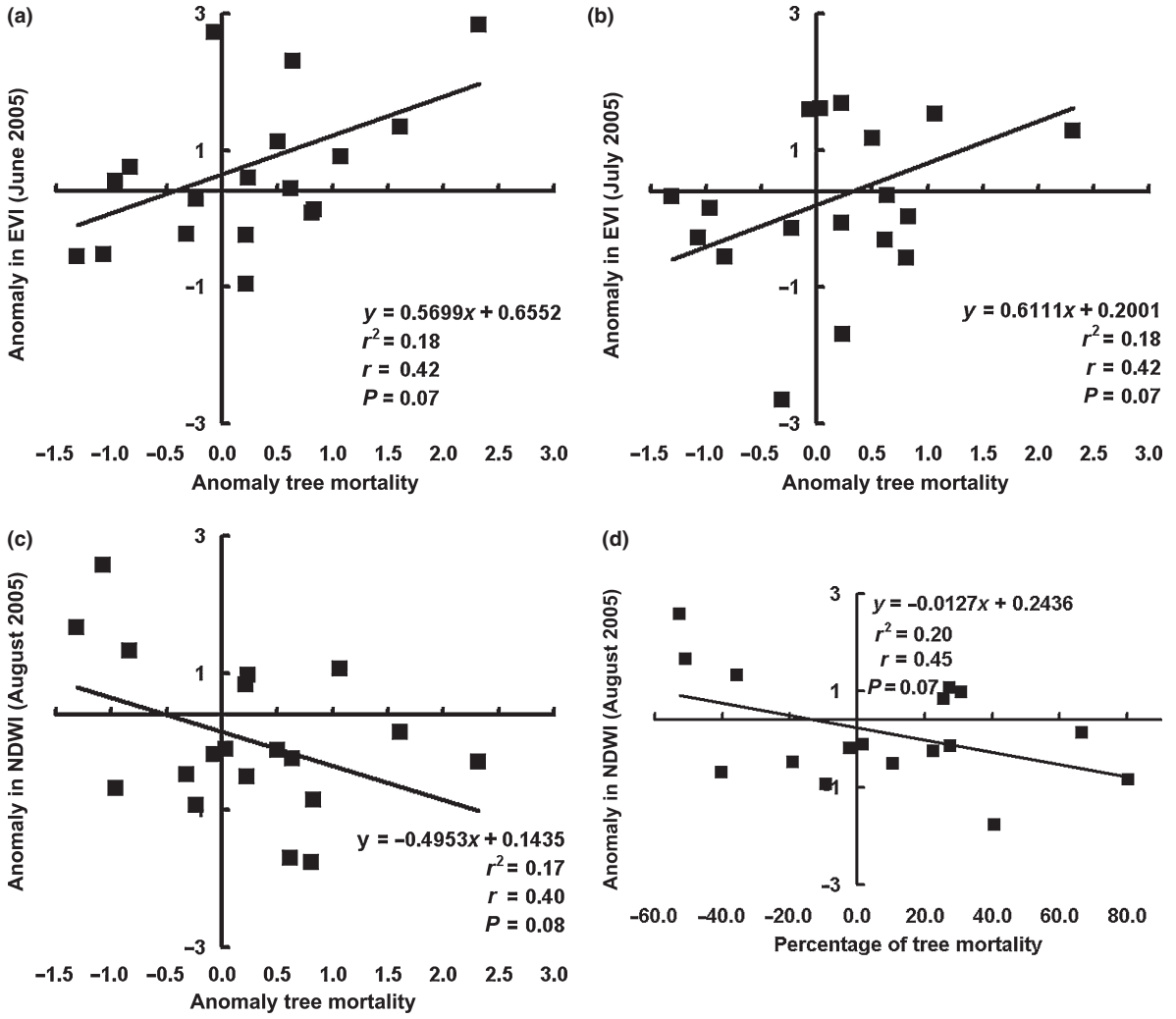

Fig. 8 Correlation indices for monthly vegetation indices anomalies with tree mortality anomalies for 2005. Anomaly in tree mortality with (a) enhanced vegetation index (EVI) June anomaly 2005, (b) EVI July anomaly 2005 and (c) normalized difference water index (NDWI) August anomaly 2005.

Landsat images from 2003 to 2007 in the Amazon region, found persistently clearer skies in the regions that displayed an increase in the MODIS EVI in relation to nongreen-up areas. The correlation analysis between the basin-wide averaged pixels for the VIs c5 and climatological data (Table 2) showed that the EVI presented the highest coefficient of determination with radiation with 1 month lag time. Similar to these previous studies (Huete *et al.*, 2006; Myneni *et al.*, 2007), our results suggest that EVI has a negative relationship with rainfall. In addition, we found that this negative relationship has the same order of magnitude as the EVI relationship with radiation, but with 2 months time lag. Furthermore, despite using VIs derived from the same product, which implies a consistent approach for the atmospheric correction of all spectral bands, we found, at the basin-wide scale, the EVI seems to be more correlated with AOD than the two other VIs.

Spatial patterns

The increase in the EVI signal detected by VIs c4 during the dry season (Huete *et al.*, 2006 and Xiao *et al.*, 2006) and during the 2005 drought (Saleska *et al.*, 2007) have been associated with the flushing of new leaves because of its positive relationship with the gross primary production (GPP) derived from tower measurements in two Amazonian sites (Huete *et al.*, 2006). The leaf flushing could potentially lead to an increase of the area-averaged canopy photosynthetic capacities (Rahman *et al.*, 2005) during the light-rich dry season (Huete *et al.*, 2006) and leaf abscission would take place during the cloudy wet season (Myneni *et al.*, 2007), although both processes can be simultaneous in many tropical trees. These studies assumed that areas that green-up correspond to regions where trees are able to use deep roots and hydrological redistribution to

maintain water availability during dry periods (Nepstad *et al.*, 1994; da Rocha *et al.*, 2004; Oliveira *et al.*, 2005).

Although large regions encompassing central, east and western Amazon forests were detected having an increase in the vegetation response (Huete *et al.*,2006; Myneni *et al.*, 2007), the onset of the rainy season exhibits a more variable pattern (Marengo *et al.*, 2001). These RS based-results have also been questioned because of the lack of direct field observations of canopy processes such as leaf phenology, the MODIS LAI product being very sensitive to the methods used to generate the monthly images (Poulter & Cramer, 2009) and the reported detection of a very homogeneous response of the majority of Amazonia (Huete *et al.*, 2006; Myneni *et al.*, 2007) in a region that has a high variability in climate (rainfall regimes; Liebmann & Marengo, 2001; Sombroek, 2001), dry season length (Marengo *et al.*, 2001), latitudinal radiation seasonality (Schafer *et al.*, 2002) and even greater biophysical variability (soil properties; Quesada *et al.*, 2009), topography, species composition (Sombroek, 2001; Sternberg, 2001; ter Steege *et al.*, 2006), canopy size (Barbier *et al.*, 2009), and aboveground productivity (Malhi *et al.*, 2004; Aragão *et al.*, 2009).

Samanta *et al.* (2010) could not reproduce the spatial patterns detected by Saleska *et al.* (2007) using the EVI c4 with a different time-series. In this study, the c4 results for the EVI anomalies correspond overall to the patterns reported by Saleska *et al.* (2007). The EVI c5 anomalies observed in this study had lower amplitude and the regions showing positive anomalies were smaller than those identified by the c4 study of Saleska *et al.* (2007). These indices, as suggested by Samanta *et al.* (2010), show that the differences between c5 and c4 results are caused by the improvements in the c5 algorithm. However, we also detected smaller regions than Samanta *et al.* (2010). This is likely to be related to the range of values defining the significant intervals used for depicting anomalous values in the time series and/or to the length of the time-series used in their study.

Positive anomalies in EVI from March to May 2005 could be related to the rainfall deficiency that affected the region in the late rainy season of 2004 (November onwards) (Marengo *et al.*, 2008). Negative anomalies from September to December 2005 in EVI and NDVI (Figs 5, S4, respectively) could be evidence of a delayed effect of the 2005 drought event. For example, in tropical (Phillips *et al.*, 2010) and in temperate zones (Bréda *et al.*, 2006), time lag between drought and tree decline has been observed, and a NDVI time lag of up to 6 months has been reported elsewhere (Salinas-Zavala *et al.*, 2002).

The SWIR-based vegetation indices track growth pattern in crops better than other indices (Chen *et al.*, 2005) and it has been shown that the these spectral bands are very sensitive to canopy structural changes and architectural parameters (Eklundh *et al.*, 2001). It has also been demonstrated that NDWI is highly sensitive to LAI (Zarco-Trejada *et al.*, 2003); this could explain the very strong correlation between NDWI and radiation in a relatively large area observed in this study.

Tree mortality

Ground-based direct measurements have shown that across South American tropical forests, litterfall seasonality is significantly and positively spatially correlated with rainfall seasonality (Chave *et al.*, 2010) with a greater litter production during the dry season (Luizão, 1989; Chave *et al.*, 2010). During severe droughts in the Amazon, effects such as a decline in leaf area (Nepstad *et al.*, 1994; Vourlitis *et al.*, 2001) and an increase in large tree mortality have been reported (Nepstad *et al.*, 2007; Phillips *et al.*, 2009; da Costa *et al.*, 2010).

Despite being only moderately significant, our correlation analysis between anomalies in EVI and tree mortality demonstrated that areas with positive EVI anomalies for the critical months of the drought period tended to occur where forest plots had higher tree mortality in 2005. The opposite trend is observed for NDWI anomalies: sites with higher tree mortality rates in 2005 tended to have lower NDWI anomalies. These results show very clearly that these forests were not thriving in the drought. We suggest instead that the apparent changes reflect structural changes in the forests affected by drought. Emergent and large trees are the most susceptible to droughts (Nepstad *et al.*, 2007; Phillips *et al.*, 2009) and to minimize water stress some are deciduous in a normal dry season (Borchert, 1998). The combined effect of dead stems and leafless trees is very likely to reduce the heterogeneity of canopy reflectance and decrease the effect of shadows cast by the highest trees. It is likely that many other trees have also dropped their leaves during the drought period but did not die in the aftermath. Hence, the EVI response could be related to the structural change (i.e. decrease of shadows) giving the opposite pattern to that normally observed.

There is evidence in the literature to support this theory. For example, it has been observed that in high spatial resolution images, red and NIR spectral bands are highly sensitive to subpixel shadow (Asner & Warner, 2003). A sensitivity analysis using a light canopy interaction model highlighted the link between canopy structure and reflectance (Gerard, 2003). In Landsat data, shade fraction was found to be highly correlated with LAI (Aragão *et al.*, 2005), and to be sensitive to change in the vegetation structure (Lu *et al.*, 2003). Finally, the decrease of the shade fraction resulting from the seasonality of emergent trees seems to directly increase the vegetation index response (Anderson *et al.*, 2010).

By contrast, the NDWI appears to directly pick up the drought effects on the canopy. The relationships between MODIS NDWI and vegetation water content have been

demonstrated in the literature (Chen *et al.*, 2005; Cheng *et al.*, 2007; Houborg *et al.*, 2007). In this study, the spatial pattern of positive anomalies in the NDWI in 2005 may be related to the detection of the lower canopy layers which did not suffer with water stress to the same intensity as the emergent trees. An indication of this process is the trend in the correlation of this index with the tree mortality data, where lower NDWIs were observed in areas with higher tree mortality.

Conclusions

We have shown that climatological and the VI derived from remotely sensed data exhibited anomalous responses during the 2005 drought in Amazonia. In addition to having evaluated a large number of remote sensing datasets with the same temporal coverage, we combined field measurements with satellite-derived VI in order to understand how these two sets of data can be interpreted together. The analysis of the vegetation indices and tree mortality data suggested that sites with higher absolute mortality rates in 2005 tend to have positive EVI anomalies and negative NDWI anomalies. This calls into question previous interpretations of these VIs as indicating increased leaf area and forest productivity, and show that positive EVI anomalies do not indicate insensitivity to droughts in Amazonian forests.

Acknowledgements

The first author thanks the Coordenação de Aperfeiçoamento de Pessoal de Nível Superior (CAPES) for the PhD scholarship (BEX4018052) and Instituto Internacional de Educação do Brasil (BECA-B/2006/01/BDE/04) for the financial support. We thank colleagues in the RAINFOR network for the collection of tree mortality data employed in this analysis. Fieldwork and plot data management was supported by NERC and the Gordon and Betty Moore Foundation. We also thank the three anonymous reviewers who contributed immensely to earlier versions of the manuscript.

References

Anderson LO, Aragão L, Shimabukuro YE, Almeida S, Huete A 2010. Use of fraction images for monitoring intra-annual phenology of different vegetation physiognomies in Amazonia. *International Journal of Remote Sensing*, doi: 10.1080/01431160903474921: 1–22.

Anderson LO, Malhi Y, Ladle RJ, Aragão LEOC, Shimabukuro Y, Phillips OL, Baker T, Costa ACL, Espejo JS, Higuchi N *et al.* 2009. Influence of landscape heterogeneity on spatial patterns of wood productivity, wood specific density and above ground biomass in Amazonia. *Biogeosciences* **6**: 1883–1902.

Andreae MO, Rosenfeld D, Artaxo P, Costa AA, Frank GP, Longo KM, Silva-Dias MAF. 2004. Smoking rain clouds over the Amazon. *Science* **303**: 1337–1342.

Aragão LEOC, Malhi Y, Metcalfe DB, Silva-Espejo JE, Jimenez E, Navarrete D, Almeida S, Costa ACL, Salinas N, Phillips OL *et al.* 2009. Above- and below-ground net primary productivity across ten Amazonian forests on contrasting soils. *Biogeosciences* **6**: 2759–2778.

Aragão L, Malhi Y, Roman-Cuesta RM, Saatchi S, Anderson LO, Shimabukuro YE. 2007. Spatial patterns and fire response of recent Amazonian droughts. *Geophysical Research Letters* **34**: 5.

Aragão L, Shimabukuro YE, Santo F, Williams M. 2005. Spatial validation of the collection 4 MODIS LAI product in Eastern Amazonia. *IEEE Transactions on Geoscience and Remote Sensing* **43**: 2526–2534.

Asner GP, Alencar A. 2010. Drought impacts on the Amazon forest: the remote sensing perspective. *New Phytologist*, doi: 10.1111/j.1469-8137.2010.03310.x.

Asner GP, Carlson KM, Martin RE. 2005. Substrate age and precipitation effects on Hawaiian forest canopies from spaceborne imaging spectroscopy. *Remote Sensing of Environment* **98**: 457–467.

Asner GP, Warner AS. 2003. Canopy shadow in IKONOS satellite observations of tropical forests and savannas. *Remote Sensing of Environment* **87**: 521–533.

Barbier N, Couteron P, Proisy C, Malhi Y, Gastellu-Etchegorry J-P. 2009. The variation of apparent crown size and canopy heterogeneity across lowland Amazonian forests. *Global Ecology and Biogeography* **19**: 72–84.

Borchert R. 1998. Responses of tropical trees to rainfall seasonality and its long term changes. *Climatic Change* **39**: 381–393.

Bréda N, Huc R, Granier A, Dreyer E. 2006. Temperate forest trees and stands under severe drought: a review of ecophysiological responses, adaptation processes and long-term consequences. *Annals of Forest Science* **63**: 625–644.

Câmara G, Valeriano DM, Soares JV. 2006. *Metodologia para o Cálculo da Taxa Anual de Desmatamento na Amazônia Legal*. São José dos Campos, SP: Instituto Nacional de Pesquisas Espaciais, 24 pages.

Carreiras JMB, Pereira JMC, Shimabukuro YE, Stroppiana D. 2003. Evaluation of compositing algorithms over the Brazilian Amazon using SPOT-4 VEGETATION data. *International Journal of Remote Sensing* **24**: 3427–3440.

Ceballos JC, Bottino MJ, de Souza JM. 2004. A simplified physical model for assessing solar radiation over Brazil using GOES 8 visible imagery. *Journal of Geophysical Research* **109**: D02211. doi:10.1029/2003JD003531

Chave J, Navarrete D, Almeida S, Álvarez E, Aragão LEOC, Bonal D, Châtelet P, Silva Espejo J, Goret JY, von Hildebrand P *et al.* 2010. Regional and temporal patterns of litterfall in tropical South America. *Biogeosciences* **7**: 43–55.

Chen D, Huang J, Jackson TJ. 2005. Vegetation water content estimation for corn and soybeans using spectral indices derived from MODIS near- and short-wave infrared bands. *Remote Sensing of Environment* **98**: 225–236.

Cheng Y-B, Wharton S, Ustin SL, Zarco-Tejada PJ, Falk M, U KTP. 2007. Relationships between moderate resolution imaging spectroradiometer water indexes and tower flux data in an old growth conifer forest. *Journal of Applied Remote Sensing* **1**: 013513–013526.

da Costa ACL, Galbraith D, Almeida S, Portela BTT, da Costa M, de Athaydes Silva Junior J, Braga AP, de Gonçalves PHL, de Oliveira AAR, Fisher R *et al.* 2010. Effect of 7 yr of experimental drought on vegetation dynamics and biomass storage of an eastern Amazonian rainforest. *New Phytologist* **187**: 579–591.

Cox PM, Harris PP, Huntingford C, Betts RA, Collins M, Jones CD, Jupp TE, Marengo JA, Nobre CA. 2008. Increasing risk of Amazonian drought due to decreasing aerosol pollution. *Nature* **453**: 212–215.

Di L. 1991. Regional-scale soil moisture monitoring using NOAA/AVHRR data. ETD collection for University of Nebraska – Lincoln. Paper AAI9129546 [WWW document]. URL http://digitalcommons.unl.edu/dissertations/AAI9129546 [accessed on 30 June 2010].

Didan K, Huete A. 2006. MODIS vegetation index product series collection 5 change summary. In: *MODIS VI C5 changes*. 17 [WWW document]. URL http://modland.nascom.nasa.gov/QA_WWW/forPage/MOD13_VI_C5_Changes_Document_06_28_06.pdf [accessed on 30 June 2010].

Eklundh LH, Harris L, Kuusk A. 2001. Investigating relationships between Landsat ETM+ sensor data and leaf area index in a boreal conifer forest. *Remote Sensing of Environment* **78**: 239–251.

Eva HD, Belward ASB, Miranda ED, Bella CM, Gond V, Hubber O, Jones S, Sgrenzaroli M, Fritz S. 2004. A land cover map of South America. *Global Change Biology* **10**: 731–744.

Gao BC. 1996. NDWI – A Normalized Difference Water Index for remote sensing of vegetation liquid water from space. *Remote Sensing of Environment* **58**: 257–266.

Gerard F. 2003. Single angle, dual angle and multi-temporal viewing: assessing through modeling the implications for forest structure variable extraction. *International Journal of Remote Sensing* **24**: 1317–1334.

Houborg R, Soegaard H, Boegh E. 2007. Combining vegetation index and model inversion methods for the extraction of key vegetation biophysical parameters using Terra and Aqua MODIS reflectance data. *Remote Sensing of Environment* **106**: 39–58.

Hubanks PA, King MD, Platnick S, Pincus R. 2008. MODIS algorithm theoretical basis document no. ATBD-MOD-30 for level-3 global gridded [WWW document]. URL http://modis-atmos.gsfc.nasa.gov/_docs/L3_ATBD_2008_12_04.pdf [accessed on 24 June 2010].

Huete A, Didan K, Miura T, Rodriguez EP, Gao X, Ferreira LG. 2002. Overview of the radiometric and biophysical performance of the MODIS vegetation indices. *Remote Sensing of Environment* **83**: 195–213.

Huete AR, Didan K, Shimabukuro YE, Ratana P, Saleska SR, Hutyra LR, Yang WZ, Nemani RR, Myneni R. 2006. Amazon rainforests green-up with sunlight in dry season. *Geophysical Research Letters* **33**: 4.

Huete A, Justice C, Liu H. 1994. Development of vegetation and soil indexes for MODIS-EOS. *Remote Sensing of Environment* **49**: 224–234.

Huete A, Justice C, van Leeuwen W. 1999. *MODIS Vegetation index (MOD 13) algorithm theoretical basis document* [WWW document]. URL http://modis.gsfc.nasa.gov/data/atbd/atbd_mod13.pdf [accessed on 24 June 2010].

INPE. 2002. PRODES digital methodology. In: *Program for the estimation of gross deforestation in the Brazilian Amazon (PRODES)*.

Justice CO, Eck TF, Tanré D, Holben BN. 1991. The effect of water vapour on the normalized difference vegetation index derived for the Sahelian region from NOAA AVHRR data. *International Journal of Remote Sensing* **12**: 1165–1187.

Justice CO, Townshend JRG, Vermote EF, Masuoka E, Wolfe RE, Saleous N, Roy DP, Morisette JT. 2002. An overview of MODIS Land data processing and product status. *Remote Sensing of Environment* **83**: 3–15.

Koltunov A, Ustin SL, Asner GP, Fung I. 2009. Selective logging changes forest phenology in the Brazilian Amazon: evidence from MODIS image time series analysis. *Remote Sensing of Environment* **113**: 2431–2440.

Koren I, Kaufman YJ, Remer LA, Martins JV. 2004. Measurement of the effect of Amazon smoke on inhibition of cloud formation. *Science* **303**: 1342–1345.

Koren I, Remer LA, Longo K. 2007. Reversal of trend of biomass burning in the Amazon. *Geophysical Research Letters* **34**: L20404. doi:10.1029/2007GL031530.

Lee J, Wong DWS. 2001. *Statistical analysis with ArcView GIS*. Hoboken, NJ, USA: John Wiley and Sons, Inc.

Lewis SL, Phillips OL, Sheil D, Vinceti B, Baker TR, Brown S, Graham AW, Higuchi N, Hilbert DW, Laurance WF *et al.* 2004. Tropical forest tree mortality, recruitment and turnover rates: calculation, interpretation, and comparison when census intervals vary. *Journal of Ecology* **92**: 929–944.

Li WH, Fu R, Dickinson RE. 2006. Rainfall and its seasonality over the Amazon in the 21st century as assessed by the coupled models for the IPCC AR4. *Journal of Geophysical Research-Atmospheres* **111**: D02111. doi:10.1029/2005JD006355.

Liang S. 2004. *Quantitative remote sensing of land surfaces*. Hoboken, NJ, USA: John Wiley & Sons, Inc.

Liebmann B, Marengo JA. 2001. Interannual variability of the rainy season and rainfall in the Brazilian Amazon Basin. *Journal of Climate* **14**: 4308–4318.

Lu D, Moran E, Batistella M. 2003. Linear mixture model applied to Amazonian vegetation classification. *Remote Sensing of Environment* **87**: 456–469.

Luizão FJ. 1989. Litter production and mineral element input to the forest floor in a Central Amazonian forest. *GeoJournal* **19**: 407–417.

Malhi Y, Baker TR, Phillips OL, Almeida S, Alvarez E, Arroyo L, Chave J, Czimczik CI, Di Fiore A, Higuchi N *et al.* 2004. The above-ground coarse wood productivity of 104 Neotropical forest plots. *Global Change Biology* **10**: 563–591.

Malhi Y, Phillips OL, Baker T, Almeida S, Fredericksen T, Grace J, Higuchi N, Killeen T, Laurance WF, Leano C *et al.* 2002. An international network to understand the biomass and dynamics of Amazonian forests (RAINFOR). *Journal of Vegetation Science* **13**: 439–450.

Marengo JA, Liebmann B, Kousky VE, Filizola NP, Wainer IC. 2001. Onset and end of the rainy season in the Brazilian Amazon Basin. *Journal of Climate* **14**: 833–852.

Marengo JA, Nobre CA, Tomasella J, Oyama MD, Sampaio de Oliveira G, de Oliveira R, Camargo H, Alves LM, Brown IF. 2008. The drought of Amazonia in 2005. *Journal of Climate* **21**: 495–516.

MODIS Reprojection Tool (MRT), version 4.0. 2008. Land Processes DAAC USGS Center for Earth Resources Observation and Science (EROS) in collaboration with the South Dakota School of Mines and Technology (SDSM&T) [WWW document]. URL https://lpdaac.usgs.gov/lpdaac/tools/modis_reprojection_tool [accessed on 30 June 2010].

Myneni RB, Yang W, Nemani RR, Huete AR, Dickinson RE, Knyazikhin Y, Didan K, Fu R, Negron Juarez RI, Saatchi SS *et al.* 2007. Large seasonal swings in leaf area of Amazon rainforests. *Proceedings of the National Academy of Sciences, USA* **104**: 4820–4823.

NASA. 2006. Tropical rainfall measuring mission (TRMM) and other data. Product 3B-43 [WWW document]. URL http://trmm.gsfc.nasa.gov/3b43.html [accessed on 30 June 2010].

Nepstad DC, Decarvalho CR, Davidson EA, Jipp PH, Lefebvre PA, Negreiros GH, Dasilva ED, Stone TA, Trumbore SE, Vieira S. 1994. The role of deep roots in the hydrological and carbon cycles of Amazonian forests and pastures. *Nature* **372**: 666–669.

Nepstad DC, Moutinho P, Dias MB, Davidson E, Cardinot G, Markewitz D, Figueiredo R, Vianna N, Chambers J, Ray D *et al.* 2002. The effects of partial throughfall exclusion on canopy processes, aboveground production, and biogeochemistry of an Amazon forest. *Journal of Geophysical Research-Atmospheres* **107**: 18.

Nepstad DC, Tohver IM, Ray D, Moutinho P, Cardinot G. 2007. Mortality of large trees and lianas following experimental drought in an Amazon forest. *Ecology* **88**: 2259–2269.

Oliveira RS, Bezerra L, Davidson EA, Pinto F, Klink CA, Nepstad DC, Moreira A. 2005. Deep root function in soil water dynamics in cerrado savannas of central Brazil. *Functional Ecology* **19**: 574–581.

Phillips OL, Aragão LEOC, Lewis SL, Fisher JB, Lloyd J, Lopez-Gonzalez G, Malhi Y, Monteagudo A, Peacock J, Quesada CA *et al.* 2009. Drought sensitivity of the Amazon rainforest. *Science* **323**: 1344–1347.

Phillips OL, Heijden G, Lewis S, Lopes-Gonzale G, Aragao LEOC, Lloyd JJ, Malhi Y, Monteagudo A, Almeida S, Davila EA *et al.* 2010. Drought-mortality relationships for tropical forests. *New Phytologist* doi: 10.1111/j.1469-8137.2010.03359.x.

Poulter B, Cramer W. 2009. Satellite remote sensing of tropical forest canopies and their seasonal dynamics. *International Journal of Remote Sensing* **30**: 6575–6590.

Quesada CA, Lloyd J, Schwarz M, Baker TR, Phillips OL, Patiño S, Czimczik C, Hodnett MG, Herrera R, Arneth A *et al.* 2009. Regional and large-scale patterns in Amazon forest structure and function are mediated by variations in soil physical and chemical properties. *Biogeosciences Discussions* **6**: 3993–4057.

Rahman AF, Sims DA, Cordova VD, El-Masri BZ. 2005. Potential of MODIS EVI and surface temperature for directly estimating per-pixel ecosystem C fluxes. *Geophysical Research Letters* **32**: L19404. doi:10.1029/2005GL024127.

Roberts DA, Green RO, Adams JB. 1997. Temporal and spatial patterns in vegetation and atmospheric properties from AVIRIS. *Remote Sensing of Environment* **62**: 223–240.

da Rocha HR, Goulden ML, Miller SD, Menton MC, Pinto LDVO, de Freitas HC, e Silva Figueira AM. 2004. Seasonality of water and heat fluxes over a tropical forest in eastern Amazonia. *Ecological Applications* **14**: 22–32.

Saleska SR, Didan K, Huete AR, da Rocha HR. 2007. Amazon forests green-up during 2005 drought. *Science* **318**: 612. doi: 10.1126/science.1146663.

Salinas-Zavala CA, Douglas AV, Dias HF. 2002. Interannual variability of NDVI in northwest Mexico. Associated climatic mechanisms and ecological implications. *Remote Sensing of Environment* **82**: 417–430.

Samanta A, Ganguly S, Hashimoto H, Devadiga S, Vermote E, Knyazikhin Y, Nemani RR, Myneni RB. 2010. Amazon forests did not green-up during the 2005 drought. *Geophysical Research Letters* **37**: L05401. doi:10.1029/2009GL042154.

Schafer JS, Holben BN, Eck TF, Yamasoe MA, Artaxo P. 2002. Atmospheric effects on insolation in the Brazilian Amazon: observed modification of solar radiation by clouds and smoke and derived single scattering albedo of fire aerosols. *Journal of Geophysical Research* **107**: 8074. doi:10.1029/2001JD000428.

Sheil D, May R. 1996. Mortality and recruitment rate evaluations in heterogeneous tropical forests. *Journal of Ecology* **84**: 91–100.

Sombroek W. 2001. Spatial and temporal patterns of Amazon rainfall. *AMBIO: A Journal of the Human Environment* **30**: 388–396.

ter Steege H, Pitman NCA, Phillips OL, Chave J, Sabatier D, Duque A, Molino JF, Prevost MF, Spichiger R, Castellanos H *et al.* 2006. Continental-scale patterns of canopy tree composition and function across Amazonia. *Nature* **443**: 444–447.

Sternberg LDSL. 2001. Savanna-forest hysteresis in the tropics. *Global Ecology & Biogeography* **10**: 369–378.

Tucker CJ. 1979. Red and photographic infrared linear combinations for monitoring vegetation. *Remote Sensing of Environment* **8**: 127–150.

Vancutsem C, Defourny P. 2009. A decision support tool for the optimization of compositing parameters. *International Journal of Remote Sensing* **30**: 41–56.

Vourlitis GL, Priante-Filho N, Hayashi MMS, Nogueira JdS, Caseiro FT, Campelo JH. 2001. Seasonal variations in the net ecosystem CO_2 exchange of a mature Amazonian transitional tropical forest (cerradão). *Functional Ecology* **15**: 388–395.

Wang J, Rich PM, Price KP. 2003. Temporal responses of NDVI to precipitation and temperature in the central Great Plains, USA. *International Journal of Remote Sensing* **24**: 2345–2364.

Xiao X, Boles S, Liu JY, Zhuang DF, Liu ML. 2002. Characterization of forest types in Northeastern China, using multitemporal SPOT-4 VEGETATION sensor data. *Remote Sensing of Environment* **82**: 335–348.

Xiao X, Hagen S, Zhang Q, Keller M, Moore B. 2006. Detecting leaf phenology of seasonally moist tropical forests in South America with multi-temporal MODIS images. *Remote Sensing of Environment* **103**: 465–473.

Zarco-Tejada PJ, Ustin SL. 2001. *Modeling canopy water content for carbon estimates from MODIS data at land EOS validation sites*, IGARRS Meeting, Sydney, Australia.

Zarco-Trejada PJ, Rueda CA, Ustin SL. 2003. Water content estimation in vegetation with MODIS reflectance data and model inversion methods. *Remote Sensing of Environment* **85**: 109–124.

Supporting Information

Additional supporting information may be found in the online version of this article.

Methods S1 MODIS VI, TRMM data processing and temporal pattern results.

Fig. S1 Monthly time-series of the anomalies derived from c4 and c5 MODIS vegetation indices algorithm.

Fig. S2 Aerosol optical depth (AOD) monthly anomalies in 2005.

Fig. S3 EVI c4 monthly anomalies.

Fig. S4 Normalized difference vegetation index (NDVI) c5 monthly anomalous in 2005.

Fig. S5 Maps of maximum correlation (within 6 months time lag) between the vegetation indices anomalies and the aerosol optical depth anomalies (AOD).

Fig. S6 Maps of maximum Pearson correlation (within 6 months time lag) between normalized difference vegetation index (NDVI) anomalies and (a) rainfall anomalies and (b) radiation anomalies.

Fig. S7 Complementary time lag maps for maximum Pearson correlation coefficients analysis (within 6 months time lag).

Table S1 Equations of the correlation analysis among MODIS vegetation indices, solar radiation, and rainfall

Please note: Wiley-Blackwell are not responsible for the content or functionality of any supporting information supplied by the authors. Any queries (other than missing material) should be directed to the *New Phytologist* Central Office.